Ain Shams Engineering Journal (2015) 6, 893–911

Ain Shams University

Ain Shams Engineering Journal

www.elsevier.com/locate/asej
www.sciencedirect.com

ELECTRICAL ENGINEERING

A hybrid DE–PS algorithm for load frequency control under deregulated power system with UPFC and RFB

Rabindra Kumar Sahu *, **Tulasichandra Sekhar Gorripotu, Sidhartha Panda**

Department of Electrical Engineering, Veer Surendra Sai University of Technology (VSSUT), Burla 768018, Odisha, India

Received 28 November 2014; revised 20 February 2015; accepted 3 March 2015
Available online 25 April 2015

KEYWORDS

Load Frequency Control (LFC);
Generation Rate Constraint (GRC);
Governor Dead Band (GDB);
Differential Evolution (DE);
Unified Power Flow Controller (UPFC);
Redox Flow Battery (RFB)

Abstract In this paper, a Modified Integral Derivative (MID) controller is proposed for Load Frequency Control (LFC) of multi-area multi-source power system in deregulated environment. The multi-source power system is having different sources of power generation such as thermal, hydro, wind and diesel generating units considering boiler dynamics for thermal plants, Generation Rate Constraint (GRC) and Governor Dead Band (GDB) non-linearity. The superiority of proposed hybrid Differential Evolution and Pattern Search (hDE-PS) optimized MID controller over GA and DE techniques is demonstrated. Further, the effectiveness of proposed hDE-PS optimized MID controller over Integral (I) and Integral Derivative (ID) controller is verified. Then, to further improve the system performance, Unified Power Flow Controller (UPFC) is placed in the tie-line and Redox Flow Batteries (RFBs) are considered in the first area. The performance of proposed approach is evaluated at all possible power transactions that take place in a deregulated power market.

1. Introduction

The main objective of power system control is to maintain continuous supply of power with an acceptable quality, to all the consumers in the system. The system will be in equilibrium, when there is a balance between the power demand and the power generated. There are two basic control mechanisms used to achieve reactive power balance (acceptable voltage profile) and real power balance (acceptable frequency values). In an interconnected power system a sudden load change in one area causes the deviation of frequency of all the areas. This change in frequency is to be corrected by Load Frequency Control (LFC) [1,2]. Nevertheless, the users of the electric power change the loads randomly and momentarily. It is impossible to maintain the balances between generation and load without control. So, a control system is essential to cancel the effects of the random load changes and to keep the frequency at the standard value [3].

* Corresponding author. Tel.: +91 9439702316.
E-mail addresses: rksahu123@gmail.com (R.K. Sahu), gtchsekhar@gmail.com (T.S. Gorripotu), panda_sidhartha@rediffmail.com (S. Panda).
Peer review under responsibility of Ain Shams University.

Production and hosting by Elsevier

http://dx.doi.org/10.1016/j.asej.2015.03.011

Nomenclature

apf	ACE participation factor
a_{12}	$-P_{R1}/P_{R2}$
ACE_i	area control error of area i
B_i	Frequency bias parameter of area i (p.u.MW/Hz)
cpf_{mn}	contract participation factor between mth $GENCO$ and nth $DISCO$
CR	crossover probability
DPM	$DISCO$ participation matrix
F	nominal system frequency (Hz)
FC	step size
G	number of generation
GDB	governor dead band
GRC	generation rate constraint
i	subscript referred to area i (1, 2)
K_{diesel}	gain of diesel unit
K_{ri}	steam turbine reheat constant of area i
K_{RFB}	gain of Redox Flow Battery
K_{PSi}	power system gain of area i (Hz/p.u.MW)
N_P	number of population size
P_{Ri}	rated power of area i (MW)
t_{sim}	simulation time (s)
T_{ri}	steam turbine reheat time constant of area i (s)
T_{Gi}	speed Governor time constant for thermal unit of area i (s)
T_{GHi}	hydro turbine speed governor main servo time constant of area i (s)
T_{PSi}	power system time constant of area i (s)
T_{RFB}	time constant of Redox Flow Battery (s)
T_{RHi}	hydro turbine speed governor transient droop time constant of area i (s)
T_{RSi}	hydro turbine speed governor reset time of area i (s)
T_{Ti}	steam turbine time constant of area i (s)
T_{UPFC}	time constant of UPFC (s)
T_{Wi}	nominal starting time of water in penstock of area i (s)
T_{12}	synchronizing coefficient between areas 1 and 2 (p.u.)
ΔF_i	incremental change in frequency of area i (Hz)
ΔP_{D_i}	incremental step load change of area i
ΔP_{Tie}	incremental change in tie-line power between areas 1 and 2 (p.u.)
$\Delta P_{Tie,12}^{actual}$	change in actual tie-line power (p.u.MW)
$\Delta P_{Tie,12}^{error}$	change in tie-line power error (p.u.MW)
$\Delta P_{Tie,12}^{scheduled}$	change in scheduled steady state tie-line power (p.u.MW)

In a traditional power system configuration, generation, transmission and distribution of an electrical power are owned by a single entity called as Vertically Integrated Utility (VIU), which supplies power to the customers at regulated tariff. In an open energy market, Generating Companies (GENCOs) may or may not participate in the LFC task as they are independent power utilities. On the other hand, Distribution Companies (DISCOs) may contract with GENCOs or Independent Power Producers (IPPs) for the transaction of power in different areas [4]. Thus, in deregulated environment, control is greatly decentralized and Independent System Operators (ISOs) are responsible for maintaining the system frequency and tie-line power flows [4,5].

The researchers in the world over are trying to propose several strategies for LFC of power systems under deregulated environment in order to maintain the system frequency and tie-line flow at their scheduled values during normal operation and also during small perturbations. Recently, Parmar et al. [6] have studied the multi-source power generation in deregulated power environment using optimal output feedback controller. Debbarma et al. [7] have proposed AGC of multi-area thermal power systems under deregulated power environment considering reheat turbines and GRC, where the fractional order PID controller parameters are optimized employing Bacterial Foraging (BF) optimization technique and the results are compared with classical controller to show its superiority. Demiroren and Zeynelgil [8] have suggested AGC in three area power system after deregulation and used GA technique to find the optimal integral gains and bias factors. A four area power system in a deregulated environment has been examined in [9]. Hybrid particle swarm optimization is used to obtain optimal gain of PID controller. However, in the above literatures the effect of physical constraints such as Generation Rate Constraint (GRC) and Governor Dead Band (GDB) nonlinearity is not examined which needs further comprehensive study.

Several classical controllers structures such as Integral (I), Proportional–Integral (PI), Integral–Derivative (ID), Proportional–Integral–Derivative (PID) and Integral–Double Derivative (IDD) have been explored in [10]. Tan and Zhang [11] have been proposed Two Degree of Freedom (TDF) Internal Model Control (IMC) method to tune decentralized PID type load frequency controllers for multi-area power systems in deregulated power environments. Liu et al. [12] have been suggested optimal Load Frequency Control (LFC) under restructured power systems with different market structures. It is found from the literature survey that, most of the work is limited to reheat thermal plants, hydro plants and relatively lesser attention has been devoted to wind, diesel generating units. Due to insufficient power generation and environmental degradation issues, it is necessary to make use of wind energy in favorable locations [13]. Keeping in view the present power scenario, combination of multisource power generation with their corresponding participation factors is considered for the present study.

Flexible AC Transmission Systems (FACTS) controllers play a crucial role to control the power flow in an interconnected power system. Several studies have explored the potential of using FACTS devices for better power system control since it provides more flexibility. Unified Power Flow Controller (UPFC) is one of the most versatile FACTS controllers which is connected in series with the transmission line or in a tie-line to improve the damping of oscillations [14]. Redox Flow Batteries (RFBs) are an active power source which can be essential not only as a fast energy compensation

device for power consumptions of large loads, but also as a stabilizer of frequency oscillations [15–17]. The RFB will, in addition to load compensating, have other applications such as power quality maintenance for decentralized power supplies. But, due to the economical reasons it is not possible to place RFB in all the areas. When UPFC and RFB are present in the system, they should act in a coordinated manner so as to control the network conditions in a very fast and economical manner.

It is obvious from the literature survey that the performance of the power system depends on the controller structure and the techniques employed to optimize the controller parameters. Hence, proposing and implementing new controller approaches using high performance heuristic optimization algorithms to real world problems are always welcome. For any meta-heuristic algorithm, a good balance between exploitation and exploration during search process should be maintained to achieve good performance. DE being a global optimizing method is designed to explore the search space and most likely gives an optimal/near-optimal solution if used alone. On the other hand, local optimizing methods like Pattern Search (PS) are designed to exploit a local area [18], but they are usually not good at exploring wide area and hence not applied alone for global optimization. Due to their respective strength and weakness, there is motivation for the hybridization of DE and PS.

In view of the above, a maiden attempt has been made in this paper to apply a hybrid DE–PS optimization technique to tune MID controller for the LFC of multi-area multi-source power systems under deregulated environment with the consideration of boiler dynamics for thermal plants, Generation Rate Constraint (GRC) and Governor Dead Band (GDB) non-linearity. The superiority of the proposed approach is shown by comparing the results with GA and DE techniques for the same power system. Additionally the dynamic performance of the system is investigated with integral and ID controllers. Further, UPFC is employed in series with the tie-line in coordination with RFB to improve the dynamic performance of the system. The effectiveness of the proposed controllers with the change in system parameters or loading conditions is assessed for the system under study. It is observed that the proposed controllers are robust and need not be retuned when the system is subjected to wide variation in system parameter and loading condition. Finally, demonstrating the ability of the proposed approach under random load perturbation has been investigated.

2. Material and method

2.1. System under study

Load Frequency Control (LFC) provides the control only during normal changes in load which are small and slow. So the nonlinear equations which describe the dynamic behavior of the system can be linearized around an operating point during these small load changes and a linear incremental model can be used for the analysis thus making the analysis simpler.

A realistic network of two-area six-unit power systems with different power generating units [19] considering the boiler dynamics for thermal plants, Generation Rate Constraint (GRC) and Governor Dead Band (GDB) non-linearity is shown in Fig. 1. Each area has a rating of 2000 MW with a nominal load of 1640 MW. Area-1 consists of reheat thermal, hydro, wind power plants and two DISCOs namely DISCO1 and DISCO2. Area-2 comprises of reheat thermal, hydro, diesel power plants and two DISCOs namely DISCO3 and DISCO4 as shown in Fig. 1. The transfer function model of wind and diesel generating units is adopted from [13]. The transfer function model of wind turbine system with pitch control is shown in Fig. 1. The model consists of hydraulic pitch actuator, data fit pitch response and blade characteristics. The diesel unit is represented by a transfer function as shown in Fig. 1. Each unit has its regulation parameter and participation factor which decide the contribution to the nominal loading, summation of participation factor of each control being equal to 1. Due to the presence of large thermal plants, their participation factor is generally large in the range of 50–60%. The participation factors of hydrounits are about 30%. As, wind and diesel generating power generations are less, their participation is usually low which is about 10–15% [19]. In the present study, participation factors for thermal and hydro are assumed as 0.575 and 0.3 respectively. For wind and diesel same participation factors of 0.125 are assumed. The nominal parameters of the system under study are given in Appendix A. The boiler dynamics configuration is incorporated in thermal plants to generate steam under pressure. This model considers the long-term dynamics of fuel and steam flow on boiler drum pressure as well as combustion controls. The block diagram of boiler dynamics [19] configuration is shown in Fig. 2. Governor dead band is defined as the total amount of a continued speed change within which there is no change in valve position. Steam turbine dead band is due to the backlash in the linkage connecting the servo piston to the camshaft. Much of this appears to occur in the rack and pinion used to rotate the camshaft that operates the control valves. Due to the governor dead band, an increase/decrease in speed can occur before the position of the valve changes. The speed governor dead band has a great effect on the dynamic performance of electric energy system. The backlash non-linearity tends to produce a continuous sinusoidal oscillation with a natural period of about 2 s. For this analysis, in this study backlash nonlinearity of 0.05% for the thermal system is considered. In a power system, power generation can change only at a specified maximum rate known as Generation Rate Constraint (GRC). Presence of GRC will affect adversely the system performance in LFC studies. Hydropower plant generating units are normally adjusted as the response is faster to raise/lower the power. Thermal power plants have rate restrictions due to thermal stresses even though all units are expected to participate in primary frequency regulation. If wind and diesel powers are available, the system performance improves with the inclusion of wind and diesel units. The improvement in the system response is due to the absence of physical constraints for wind and diesel units and they can quickly pick up the additional load demand thus stabilizing the system more quickly. In the present study, a GRC of 3% per min is considered for thermal units. The GRCs for hydrounit are 270% per minute for raising generation and 360% per minute for lowering generation are considered [19,20].

2.2. LFC in restructured scenario

The conventional AGC schemes aim to attain optimal generation allocation to the generator units. However, under

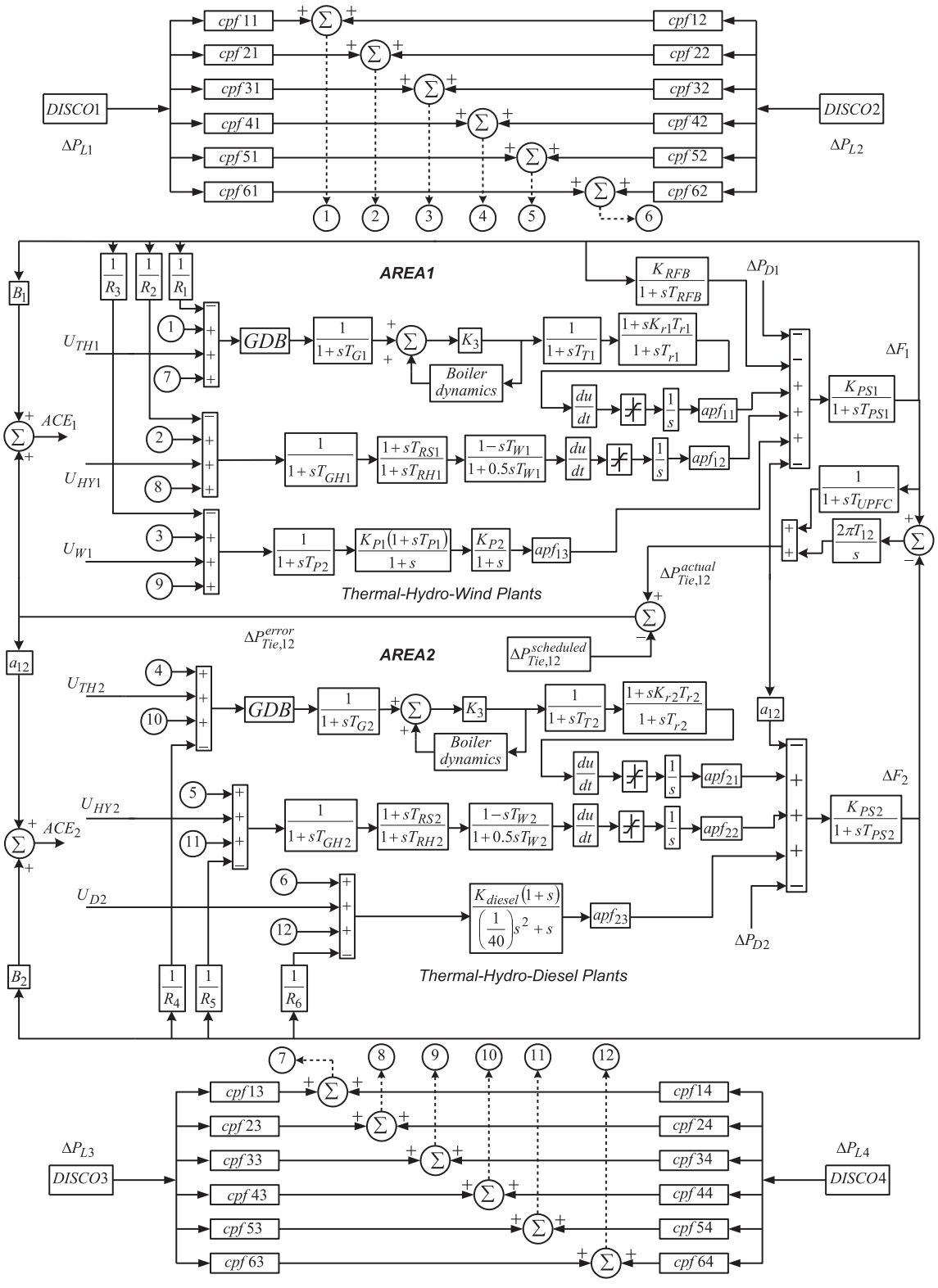

Figure 1 MATLAB/Simulink model of two-area diverse source power system under restructured scenario.

deregulation, AGC is allowed to control the contract powers of IPPs (Independent Power Producers) rather than the outputs of generation units. In deregulated environment, AGC adapts the market requirement with several kinds of the bidding strategies in order to achieve the economic optimality. All IPPs participate in electricity power bidding and provide unit prices or the incremental cost curves. Hence, in a deregulated environment, the AGC is mostly related to the bidding

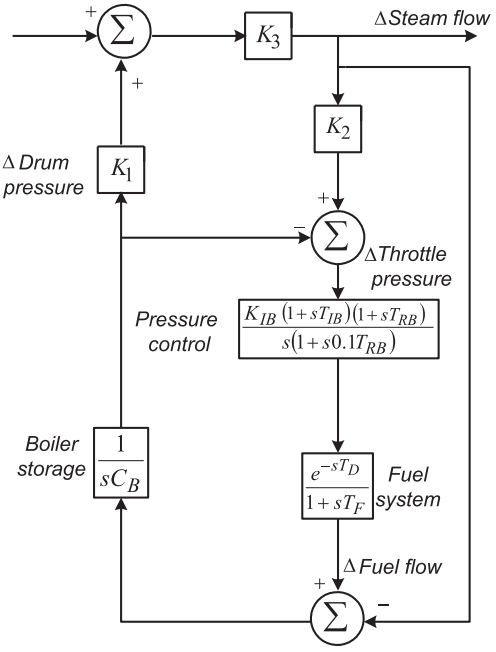

Figure 2 Block diagram of boiler dynamics configuration.

adjustment, which is performed by the market competition based on the incremental cost curves. The contract participation factors provide a compact yet precise way of summarizing contractual arrangements.

In restructured scenario, the GENCOs in one area may supply DISCOs in same area as well as DISCOs in other areas. The DISCOs have the freedom to purchase power from different GENCOs at competitive prices. The various combinations of contracts between DISCOs and GENCOs are analyzed by the concept of a DISCO Participation Matrix (DPM) [4,9]. The rows of a DPM correspond to GENCOs and columns represent to DISCOs which contract power. The corresponding DPM for the system is as follows:

$$\mathrm{DPM} = \begin{bmatrix} cpf_{11} & cpf_{12} & cpf_{13} & cpf_{14} \\ cpf_{21} & cpf_{22} & cpf_{23} & cpf_{24} \\ cpf_{31} & cpf_{32} & cpf_{33} & cpf_{34} \\ cpf_{41} & cpf_{42} & cpf_{43} & cpf_{44} \\ cpf_{51} & cpf_{52} & cpf_{53} & cpf_{54} \\ cpf_{61} & cpf_{62} & cpf_{63} & cpf_{64} \end{bmatrix} \tag{1}$$

where *cpf* represents contract participation factor. Each entry in this matrix can be thought as a fraction of a total load contracted by a *n*th-DISCO (column) toward a *m*th-GENCO (row). The sum of all the entries in a column in this matrix is unity and mathematically it can be expressed as follows:

$$\sum_{m=1}^{6} cpf_{mn} = 1 \tag{2}$$

The scheduled steady state power flow on the tie-line can be given as follows:

$$\Delta P_{Tie,12}^{scheduled} = (\text{Demand of DISCOs in area1 to GENCOs in area2}) - (\text{Demand of DISCOs in area2 to GENCOs in area1}) \tag{3}$$

Mathematically Eq. (3) can be defined as follows:

$$\Delta P_{Tie,12}^{scheduled} = \sum_{m=1}^{3}\sum_{n=3}^{4} cpf_{mn}\Delta P_{Ln} - \sum_{m=4}^{6}\sum_{n=1}^{2} cpf_{mn}\Delta P_{Ln} \tag{4}$$

The actual tie-line power can be represented as follows:

$$\Delta P_{Tie,12}^{actual} = \frac{2\pi T_{12}}{s}(\Delta F_1 - \Delta F_2) \tag{5}$$

The tie-line power error can now be expressed as follows:

$$\Delta P_{Tie,12}^{error} = \Delta P_{Tie,12}^{actual} - \Delta P_{Tie,12}^{scheduled} \tag{6}$$

$\Delta P_{Tie,12}^{error}$ reduces to zero in the steady as the actual tie-line power flow reaches the scheduled power flow. The generated power or contracted power supplied by the GENCOs is given as follows:

$$\Delta P_{gm} = \sum_{n=1}^{4} cpf_{mn} P_{Ln} \tag{7}$$

This error signal is used to generate the respective Area Control Error (*ACE*) signals during the traditional scenario as given below:

$$ACE_1 = B_1\Delta F_1 + \Delta P_{Tie,12}^{error} \tag{8}$$

$$ACE_2 = B_2\Delta F_2 + \Delta P_{Tie,21}^{error} \tag{9}$$

As there are three GENCOs in each area, *ACE* signal has to be distributed among them in proportion to their participation in the LFC. Coefficients that distribute *ACE* to GENCOs are termed as "*ACE* Participation Factors (*apf*s)". In a given control area, the sum of participation factors is equal to 1. Hence, apf_{11}, apf_{12}, apf_{13} are considered as *ACE* participation factor in area-1 and apf_{21}, apf_{22}, apf_{23} are in area-2. Participation factors for thermal and hydro are assumed as 0.575 and 0.3 respectively. For wind and diesel same participation factor of 0.125 is assumed.

2.3. Controller structure and Objective function

As the areas are assumed unequal, different Modified Integral Derivative (MID) controllers are considered for each generating unit to minimize the frequency oscillations and to control the tie-line powers. The MID control scheme is shown in Fig. 3. Design of MID controller requires determination of the two main parameters, integral time constant (K_I) and Derivative time constant (K_{DD}).

The error inputs to the controllers are the respective area control errors (ACE) given by the following:

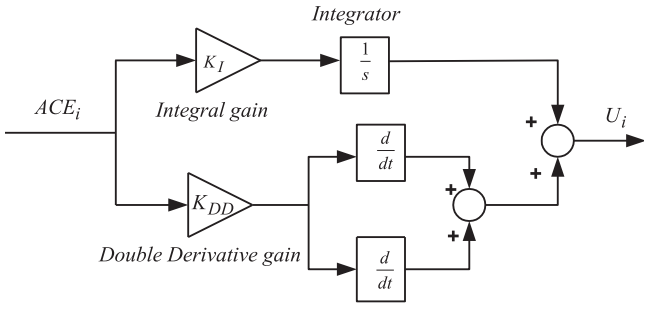

Figure 3 Structure of proposed MID controller.

$$e_1(t) = ACE_1 = B_1\Delta F_1 + \Delta P_{Tie} \quad (10)$$

$$e_2(t) = ACE_2 = B_2\Delta F_2 + a_{12}\Delta P_{Tie} \quad (11)$$

MID controller uses ACE_1 as input in area-1 and ACE_2 in area-2. In area-1, the outputs of the MID controllers U_{TH1}, U_{HY1} and U_{W1} are the control inputs of the thermal, hydro and wind generating units respectively. In area-2, the outputs of the MID controllers U_{TH2}, U_{HY2} and U_{D2} are the control inputs of the power system. The integral and derivative gains of the MID controllers are represented as K_{I1}, K_{I2}, K_{I3}, K_{I4}, K_{I5}, K_{I6}, K_{DD1}, K_{DD2}, K_{DD3}, K_{DD4}, K_{DD5} and K_{DD6} respectively.

In the design of a modern heuristic optimization technique based controller, the objective function is first defined based on the desired specifications and constraints. Performance criteria usually considered in the control design are the Integral of Time multiplied Absolute Error (ITAE), Integral of Squared Error (ISE), Integral of Time multiplied Squared Error (ITSE) and Integral of Absolute Error (IAE). ITAE criterion reduces the settling time which cannot be achieved with IAE or ISE based tuning. ITAE criterion also reduces the peak overshoot. ITSE based controller provides large controller output for a sudden change in set point which is not advantageous from controller design point of view. It has been reported that ITAE is a better objective function in LFC studies [21]. Therefore in this paper ITAE is used as objective function to optimize the MID controller. Expression for the ITAE objective function is depicted in Eq. (12).

$$J = ITAE = \int_0^{t_{sim}} (|\Delta F_1| + |\Delta F_2| + |\Delta P_{Tie}|) \cdot t \cdot dt \quad (12)$$

In the above equations, ΔF_1 and ΔF_2 are the system frequency deviations; ΔP_{Tie} is the incremental change in tie- line power; t_{sim} is the time range of simulation. The problem constraints are the MID controller parameter bounds. Therefore, the design problem can be formulated as the following optimization problem.

$$\text{Minimize } J \quad (13)$$

$$\text{Subject to } K_{I_{\min}} \leqslant K_I \leqslant K_{I_{\max}}, K_{DD_{\min}} \leqslant K_{DD} \leqslant K_{DD_{\max}} \quad (14)$$

2.4. Modeling of UPFC in LFC

During the last decade, continuous and fast improvement of power electronics technology has made Flexible AC Transmission Systems (FACTS) a promising concept for power system applications. With the application of FACTS technology, power flow along transmission lines can be more flexibly controlled. The Unified Power Flow Controller (UPFC) is regarded as one of the most versatile devices in the FACTS family which has the capability to control of the power flow in the transmission line, improve the transient stability, alleviate system oscillation and offer voltage support [14]. The two-area power system with a UPFC as shown in Fig. 4 is considered in this study. The UPFC installed in series with a tie-line and provides damping of oscillations the tie-line power [22]. In Fig. 4, V_{se} is the series voltage magnitude and ϕ_{se} is the phase angle of series voltage. The shunt converter injects controllable shunt voltage such that the real component of the current in the shunt branch balance the real power demanded by the series converter. It is clear from Fig. 4 that, the complex power at the receiving-end of the line as follows:

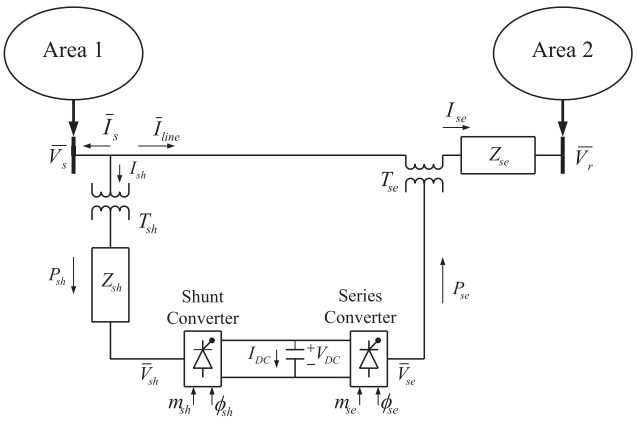

Figure 4 Two area interconnected power system with UPFC.

$$P_{real} - jQ_{reactive} = \overline{V_r^*} I_{line} = \overline{V_r^*}\left\{\frac{(\overline{V_s} + \overline{V_{se}} - \overline{V_r})}{j(X)}\right\} \quad (15)$$

where

$$\overline{V_{se}} = |V_{se}|\angle(\delta_s - \phi_{se}) \quad (16)$$

Solving Eq. (15), the real part as given below

$$P_{real} = \frac{|V_s||V_r|}{(X)}\sin(\delta) + \frac{|V_s||V_{se}|}{(X)}\sin(\delta - \phi_{se}) = P_0(\delta) + P_{se}(\delta, \phi_{se}) \quad (17)$$

The above equation, if $V_{se} = 0$, it represents that the real power is uncompensated system, whereas the UPFC series voltage magnitude can be controlled between 0 and V_{se} max, and its phase angle (ϕ_{se}) can be controlled between 0° and 360° at any power angle. The UPFC based controller can be represented in LFC as follows [23]:

$$\Delta P_{\text{UPFC}}(s) = \left\{\frac{1}{1 + sT_{\text{UPFC}}}\right\}\Delta F(s) \quad (18)$$

where T_{UPFC} is the time constant of UPFC.

2.5. Modeling of RFB in LFC

In an interconnected power system during the presence of small load perturbations and with optimized controller gains, the frequency deviations and tie-line power changes exist for long time durations. During such conditions the governor may not able to absorb the frequency deviations due to slow response and non-linearities present in the system model. Therefore, in order to reduce the frequency deviations and change in tie-line power, an active power source with quick response such as RFB can be expected to the most effective one [15,17]. The RFB is found to be superior over the other

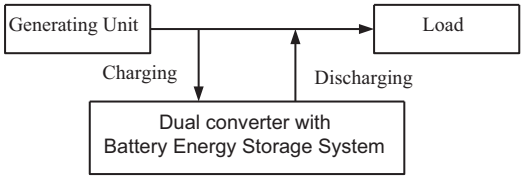

Figure 5 General block diagram of redox flow batteries in LFC.

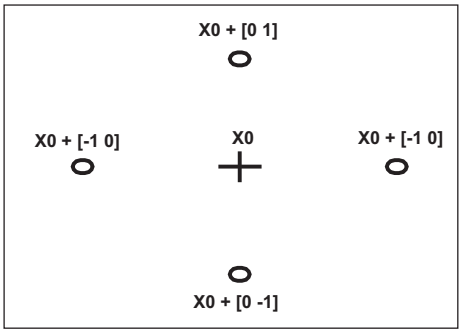

Figure 6 Pattern search mesh points and the pattern.

energy storage devices like Superconducting Magnetic Energy Storage (SMES) because of its easy operating at normal temperature, very small losses during operating conditions and has long service life [16]. However, it will be difficult to place RFB in each and every area in the interconnected power system due to the economical reasons. Since, RFB is capable of ensuring a very quick response [17], ΔF_1 is being used directly as the input command value for load frequency control. The general block diagram of the RFB used for LFC in the interconnected power system is shown in Fig. 5 [24]. During very small load duration battery charges and delivers the energy to the system during sudden load changes. The dual converter performs both rectifier and inverter action. For sudden step load perturbation the change of output of a RFB is given as [17]

$$\Delta P_{\mathrm{RFB}} = \frac{K_{\mathrm{RFB}}}{1 + sT_{\mathrm{RFB}}} \Delta F_1 \tag{19}$$

Table 1 Tuned MID controller parameters for different techniques under poolco based without UPFC and RFB.

Parameters/techniques	GA	DE	hDE-PS
K_{I1}	−0.0849	−0.3089	−1.1055
K_{I2}	−0.0051	−0.4217	−1.6300
K_{I3}	−1.2335	−1.6997	−1.7692
K_{I4}	0.3737	−0.7677	−1.7290
K_{I5}	−1.0256	−1.6481	−0.1013
K_{I6}	−0.1642	−1.0731	−0.9042
K_{DD1}	−1.7622	−1.8233	−1.6399
K_{DD2}	1.9259	1.3752	1.3061
K_{DD3}	0.2986	0.1406	−0.0958
K_{DD4}	1.0657	1.6891	1.6356
K_{DD5}	0.9175	0.9271	−1.2201
K_{DD6}	−0.0375	−0.4267	−0.2595

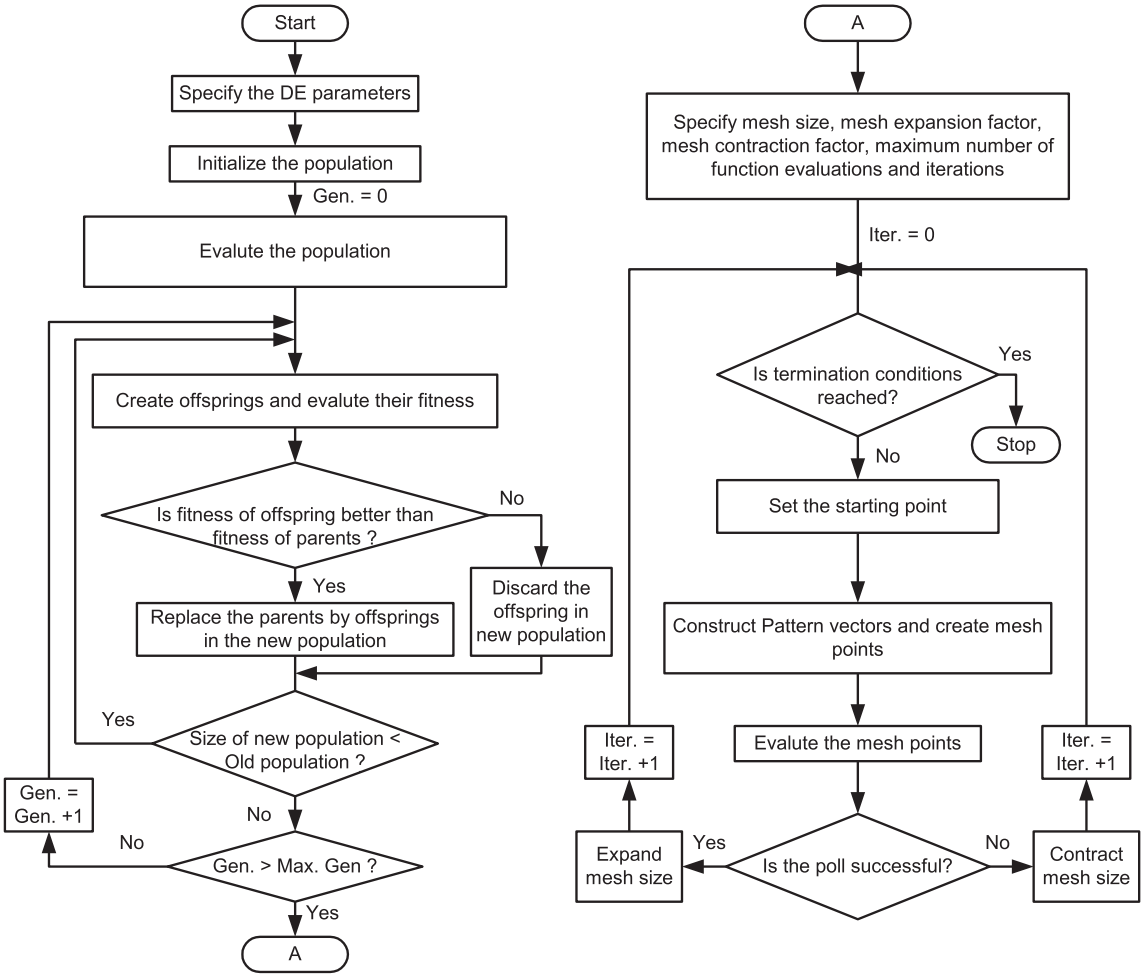

Figure 7 Flowchart of proposed Hybrid Differential Evolution Pattern Search (hDE-PS) algorithm.

Table 2 Performance index for different techniques under poolco based without UPFC and RFB.

Performance index		GA	DE	hDE-PS
ITAE		2.4264	1.8503	1.6995
Settling Time T_S (s)	ΔF_1	38.91	32.74	28.84
	ΔF_2	38.93	33.56	29.52
	ΔP_{Tie}	28.17	22.53	18.65
Peak over shoot	ΔF_1	0.0252	0.0138	0.0086
	ΔF_2	0.0032	0.0019	0.0027
	ΔP_{Tie}	0.0024	0.0019	0.0017

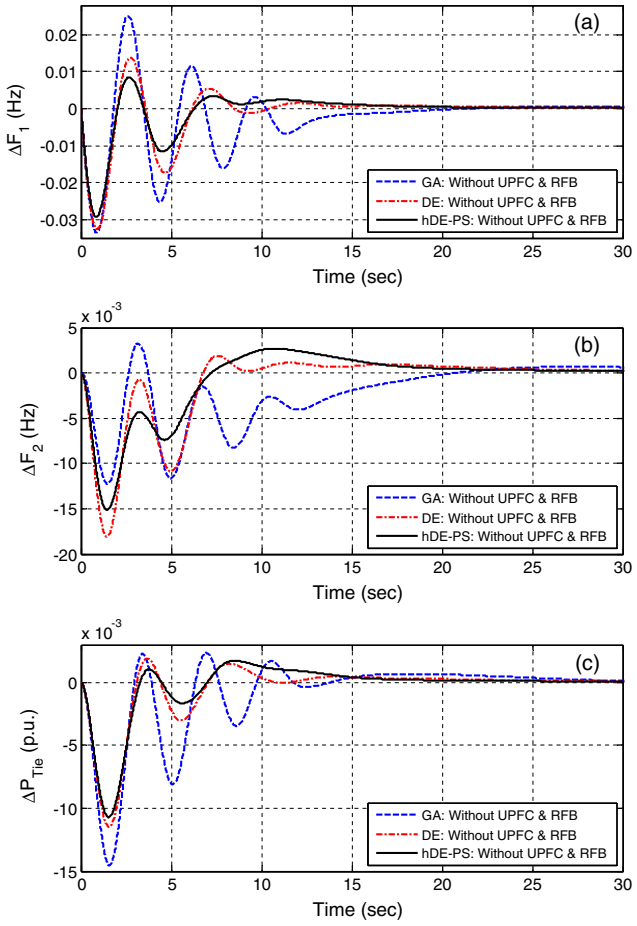

Figure 8 Dynamic responses of the system under poolco based scenario without UPFC and RFB (a) frequency deviation of area-1 (b) frequency deviation of area-2 (c) tie-line power deviation.

where K_{RFB} is gain and T_{RFB} is time constant of RFB in sec.

3. Hybrid differential evolution pattern search (hDE-PS) algorithm

To search the highly multimodal space, a two phase hybrid method known as hybrid Differential Evolution Pattern Search (hDE-PS) is employed. In this algorithm, DE is used for global exploration and the Pattern Search algorithm [18] is employed for local search. The first phase is explorative, employing a classical DE to identify promising areas of the search space. The best solution found by DE is then refined using PS method during a subsequent exploitative phase. In order to establish the superiority of proposed hDE-PS approach, the results are compared with individual DE approach. Each of these algorithms is described below.

3.1. Differential evolution

Differential Evolution (DE) algorithm is a population-based stochastic optimization algorithm recently introduced [25]. Advantages of DE are: simplicity, efficiency and real coding, easy use and speediness. DE works with two populations; old generation and new generation of the same population. The size of the population is adjusted by the parameter N_P. The population consists of real valued vectors with dimension D that equals the number of design parameters/control variables. The population is randomly initialized within the initial parameter bounds. The optimization process is conducted by means of three main operations: mutation, crossover and selection. In each generation, individuals of the current population become target vectors. For each target vector, the mutation operation produces a mutant vector, by adding the weighted difference between two randomly chosen vectors to a third vector. The crossover operation generates a new vector, called

Table 3 Tuned I/ID controller parameters for hDE-PS technique under poolco based without UPFC and RFB.

Controller Parameters	hDE-PS	
	I controller	ID controller
K_{I1}	−0.8915	−0.5559
K_{I2}	−0.8810	−0.8228
K_{I3}	−0.1314	−0.6174
K_{I4}	0.3743	0.9904
K_{I5}	0.3467	−0.9933
K_{I6}	−0.2816	−0.3666
K_{D1}	–	0.3998
K_{D2}	–	−0.4894
K_{D3}	–	−0.3730
K_{D4}	–	−0.4120
K_{D5}	–	0.1552
K_{D6}	–	−0.1477

Table 4 Performance index for different controllers under poolco based without UPFC and RFB.

Parameters		hDE-PS		
		I controller	ID controller	Proposed MID controller
ITAE		3.5887	2.8375	1.6995
T_S (s)	ΔF_1	47.47	28.79	28.84
	ΔF_2	48.18	28.51	29.52
	ΔP_{Tie}	40.45	21.47	18.65
Peak over shoot	ΔF_1	0.0102	0.0092	0.0086
	ΔF_2	0.0043	0.0036	0.0027
	ΔP_{Tie}	0.0031	0.0022	0.0017

Table 5 Tuned controller parameters and performance index for poolco based transaction with UPFC and RFB.

Parameters		With UPFC only	Both UPFC and RFB
Controller parameters	K_{I1}	−0.6411	−1.6479
	K_{I2}	−0.1536	−0.0925
	K_{I3}	−1.8266	−1.9571
	K_{I4}	−0.9767	−0.8544
	K_{I5}	−0.8065	−0.0093
	K_{I6}	−0.5210	−1.6644
	K_{DD1}	−1.3029	0.0211
	K_{DD2}	0.2109	−0.3625
	K_{DD3}	0.7704	1.7528
	K_{DD4}	−1.9062	−0.0337
	K_{DD5}	0.8197	0.8108
	K_{DD6}	−0.4898	−0.5453
Performance index with original DPM	ITAE	1.0088	0.3858
Settling time T_S (s)	ΔF_1	19.86	19.07
	ΔF_2	22.16	18.09
	ΔP_{Tie}	13.89	12.69
Peak over shoot	ΔF_1	0.0020	0.0008
	ΔF_2	0.0033	0.0017
	ΔP_{Tie}	0.0017	0.0006
Performance index with modified DPM	ITAE	1.0506	0.3868
Settling Time T_S (s)	ΔF_1	19.87	19.13
	ΔF_2	21.97	18.15
	ΔP_{Tie}	13.88	12.65
Peak over shoot	ΔF_1	0.0020	0.0007
	ΔF_2	0.0033	0.0017
	ΔP_{Tie}	0.0017	0.0006

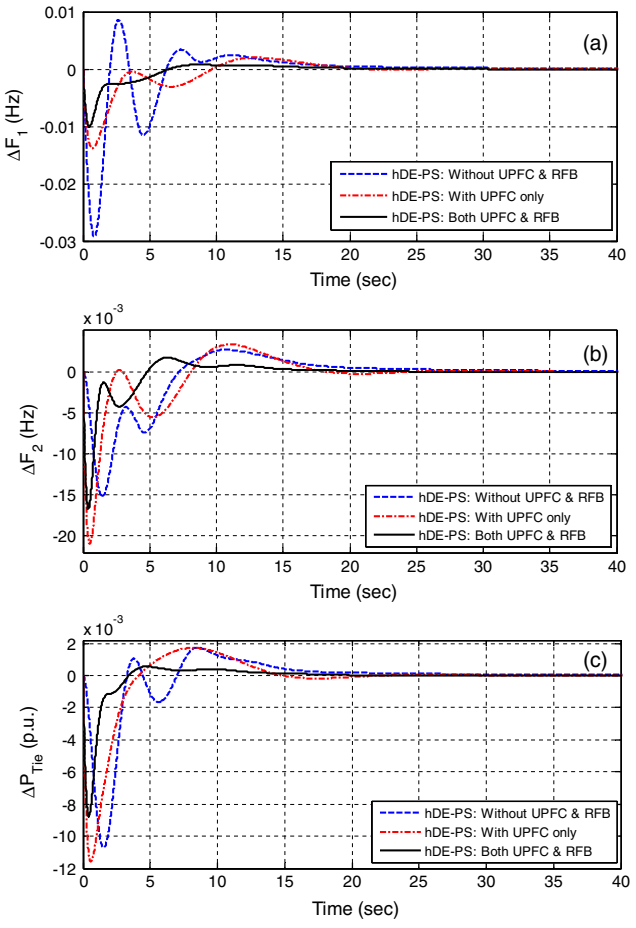

Figure 9 Dynamic responses of the system under poolco based scenario (a) frequency deviation of area-1 (b) frequency deviation of area-2 (c) tie-line power deviation.

trial vector, by mixing the parameters of the mutant vector with those of the target vector. If the trial vector obtains a better fitness value than the target vector, then the trial vector replaces the target vector in the next generation. The DE algorithm is explained in more detail in [26].

3.2. Pattern search

The Pattern Search (PS) optimization technique is a derivative free evolutionary algorithm suitable to solve a variety of optimization problems that lie outside the scope of the standard optimization methods. It is simple in concept, easy to implement and computationally efficient. It possesses a flexible and well-balanced operator to enhance and adapt the global search and fine tune local search [18]. The PS algorithm computes a sequence of points that may or may not approach to the optimal point. The algorithm starts with a set of points called mesh, around the initial points. The initial points or current points are provided by the DE technique. The mesh is created by adding the current point to a scalar multiple of a set of vectors called a pattern. If a point in the mesh is having better objective function value, it becomes the current point at the next iteration [27].

The Pattern search begins at the initial point X0 that is given as a starting point by the DE algorithm. At the first iteration, with a scalar = 1 called mesh size, the pattern vectors or direction vectors are constructed as [0 1], [1 0], [−1 0] and [0 −1]. The direction vectors are added to the initial point X0 to compute the mesh points as X0 + [0 1], X0 + [1 0], X0 + [−1 0] and X0 + [0 −1] as shown in Fig. 6. The algorithm computes the objective function at the mesh points in the same order. The algorithm polls the mesh points by computing their objective function values until it finds one whose value is smaller than the objective function value of X0. Then the poll is said to be successful when the objective function value decreases at some mesh point and the algorithm sets this point equal to X1. After a successful poll, the algorithm steps to iteration 2 and multiplies the current mesh size by 2. As the mesh size is increased by multiplying by a factor i.e. 2, this is called the expansion factor. So in 2nd iteration, the mesh points are: X1 + 2 * [0 1], X1 + 2 * [1 0], X1 + 2 * [−1 0] and X1 + 2 * [0 −1] and the process is repeated until stopping criteria is met. Now if in a particular iteration, none of the mesh points has a smaller objective function value than the value at initial/current point at that iteration, the poll is said to be unsuccessful and same current point is used in the next iteration. Also, at the next iteration, the algorithm multiplies the current mesh size by 0.5, a contraction factor, so that the mesh size at the next iteration is smaller and the process is repeated until stopping criteria is met. The flow chart of proposed hybrid Pattern Search (PS) and DE approach is shown in Fig. 7.

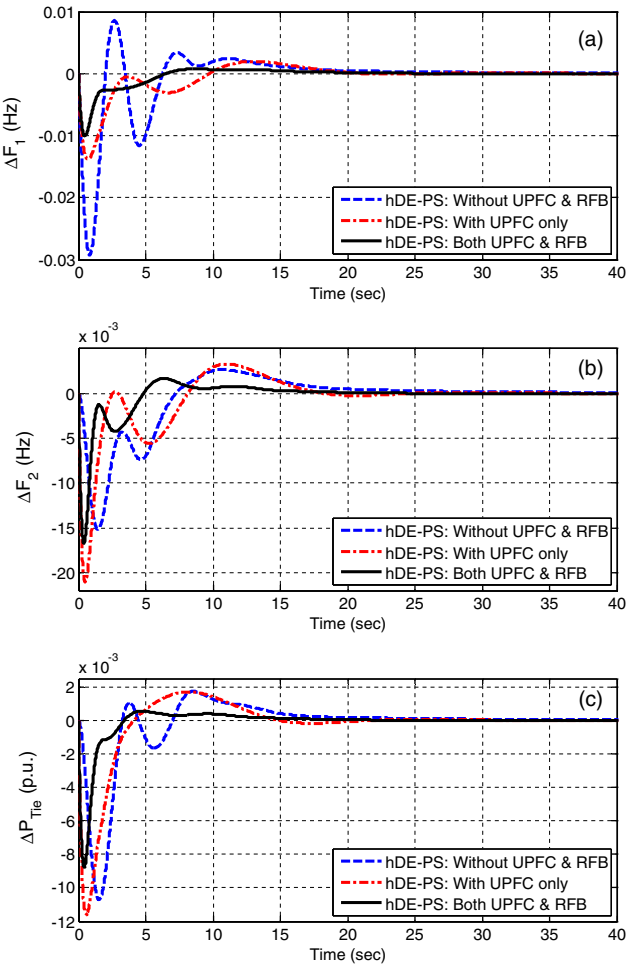

Figure 10 Dynamic responses of the system for poolco based scenario under changed contract participation factor (a) frequency deviation of area-1 (b) frequency deviation of area-2 (c) tie-line power deviation.

Table 6 Tuned MID controller parameters for bilateral based transaction.

Parameters	Without UPFC and RFB	With UPFC only	Both UPFC and RFB
K_{I1}	−1.3695	−0.3991	−1.8508
K_{I2}	−0.0009	−0.1642	−0.2280
K_{I3}	−0.6181	−1.7254	−1.7830
K_{I4}	−0.2876	−0.9905	−0.0836
K_{I5}	−1.8029	−1.1901	−0.9467
K_{I6}	−0.3662	−1.6529	−0.9800
K_{DD1}	−0.1873	0.3007	−0.0697
K_{DD2}	−1.7571	0.4249	−0.2910
K_{DD3}	−0.0644	−1.1422	1.0465
K_{DD4}	0.4916	0.0797	−0.5740
K_{DD5}	−1.6104	1.9567	1.0594
K_{DD6}	−0.7602	−0.0403	−0.2104

Table 7 Performance index values under bilateral based transaction.

Parameters		Without UPFC and RFB	With UPFC only	Both UPFC and RFB
ITAE		2.0231	1.0331	0.5033
T_S (s)	ΔF_1	31.00	22.81	20.15
	ΔF_2	38.13	21.72	18.58
	ΔP_{Tie}	32.82	13.13	14.22
Peak over shoot	ΔF_1	0.0102	0.0017	0.0010
	ΔF_2	0.0039	0.0028	0.0016
	ΔP_{Tie}	0.0028	0.0013	0.0009

4. Results and discussions

4.1. Design of proposed hybrid DE–PS optimized MID controller

The model of the system under study shown in Fig. 1 is developed in MATLAB/SIMULINK environment and hybrid DE–PS program is written (in .mfile). Initially, dissimilar MID controllers are considered for each generating unit without considering the UPFC and RFB under poolco based transaction. The control gains of MID controller are chosen in the range $[-2, 2]$. The developed model is simulated in a separate program (by .mfile using initial population/controller parameters) considering a 1% step load change (1% of nominal load i.e. 16.4 MW) in area-1. The objective function is calculated in the .mfile and used in the optimization algorithm. In the present study, a population size of $N_P = 40$, generation number $G = 30$, step size $FC = 0.2$ and crossover probability of $CR = 0.6$ have been used [26]. One more important point that more or less affects the optimal solution is the range for unknowns. For the very first execution of the program, wider solution space can be given, and after getting the solution, one can shorten the solution space nearer to the values obtained in the previous iterations. Simulations were conducted on an Intel, Core i-5 CPU of 2.5 GHz, 8 GB, 64-bit processor computer in the MATLAB 7.10.0.499 (R2010a) environment. The optimization process was repeated 20 times for DE, PS and hDE-PS algorithm. The maximum number of iteration is set to 30 for individual DE and PS techniques. In hDE-PS approach, DE technique is applied for 20 iterations and PS is then employed for 10 iterations to fine tune the best solution provided by DE. PS is executed with a mesh size of 1, mesh expansion factor of 2 and mesh contraction factor of 0.5. The maximum number of objective function evaluations is set to 10. The best final solution corresponding to the minimum fitness values obtained among the 20 runs is chosen as controller parameters. The best final solution obtained in the 20 runs is chosen as controller parameters. For the implementation of GA, normal geometric selection, arithmetic crossover and nonuniform mutation are employed in the present study. A population size of 40 and maximum generation of 30 is employed in the present paper. A detailed description about GA parameters employed in the present paper can be found in reference [8].

4.2. Poolco based transaction

In this scenario DISCOs have contract with GENCOs of the same area. It is assumed that the load disturbance occurs only

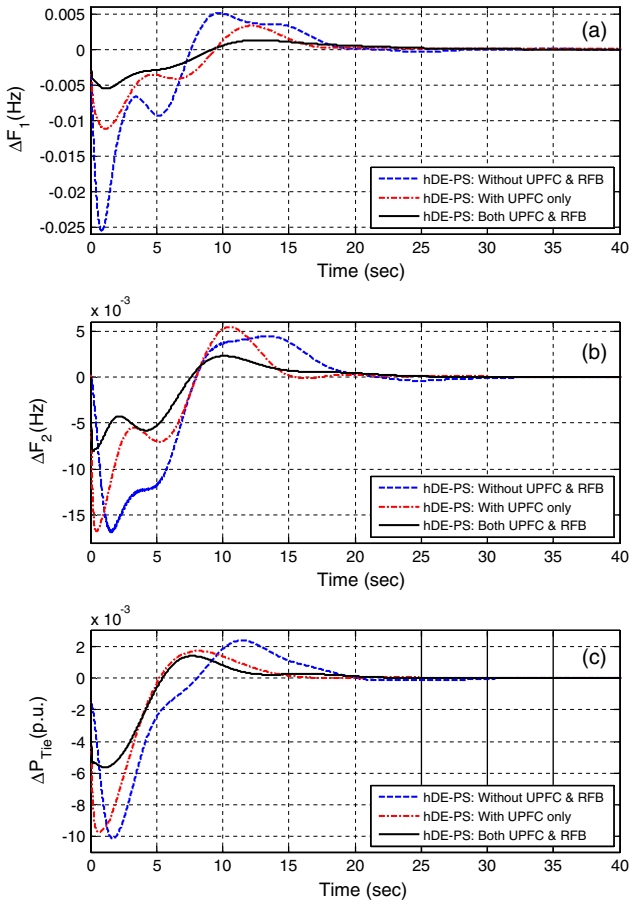

Figure 11 Dynamic responses of the system for under bilateral based scenario (a) frequency deviation of area-1 (b) frequency deviation of area-2 (c) tie-line power deviation.

Table 8 Tuned MID controller parameters for contract violation.

Parameters	Contract violation based		
	Without UPFC and RFB	With UPFC only	Both UPFC and RFB
K_{I1}	−1.4532	−1.0831	−1.6479
K_{I2}	−0.7074	−0.6858	−0.0925
K_{I3}	−1.7374	−1.9901	−1.9571
K_{I4}	−0.5481	−0.4036	−0.8544
K_{I5}	−1.1258	−0.7255	−0.0093
K_{I6}	−0.9201	−1.9699	−1.6644
K_{DD1}	−1.5026	−0.1434	0.0211
K_{DD2}	−0.7569	0.1455	−0.3625
K_{DD3}	0.0779	0.5204	1.7528
K_{DD4}	0.1016	−0.3282	−0.0337
K_{DD5}	0.2420	−1.1942	0.8108
K_{DD6}	−0.7941	−0.3701	−0.5453

in area-1. There is 0.005 (pu MW) load disturbance in DISCO1 and DISCO2, i.e. $\Delta P_{L1} = 0.005$ (pu MW), $\Delta P_{L2} = 0.005$ (pu MW), $\Delta P_{L3} = \Delta P_{L4} = 0$ (pu MW) as a result of the total load disturbance in area-1 i.e. $\Delta P_{D1} = 0.01$ (pu MW). A particular case of Poolco based contracts between DISCOs and available GENCOs is simulated based on the following DPM:

Table 9 Performance index values under contract violation.

Parameters		Without UPFC and RFB	With UPFC only	Both UPFC and RFB
ITAE		2.9831	1.8820	1.0506
T_S (s)	ΔF_1	28.26	27.77	24.31
	ΔF_2	28.65	26.30	22.72
	ΔP_{Tie}	22.40	18.68	19.05
Peak over shoot	ΔF_1	0.0302	0.0031	0.0016
	ΔF_2	0.0076	0.0057	0.0021
	ΔP_{Tie}	0.0027	0.0026	0.0010

$$\text{DPM} = \begin{bmatrix} 0.5 & 0.5 & 0 & 0 \\ 0.3 & 0.3 & 0 & 0 \\ 0.2 & 0.2 & 0 & 0 \\ 0 & 0 & 0 & 0 \\ 0 & 0 & 0 & 0 \\ 0 & 0 & 0 & 0 \end{bmatrix} \tag{20}$$

In the above case, DISCO3 and DISCO4 do not demand power from any GENCOs, and hence the corresponding contract participation factors are zero. Accordingly, the *ACE* participation of GENCOs are: $apf_{11} = apf_{21} = 0.575$, $apf_{12} = apf_{22} = 0.3$, $apf_{13} = apf_{23} = 0.125$. The scheduled tie-line power in this case is zero.

In the steady state, generation of a GENCO must match the demand of DISCOs in contract with it. The desired generation of the mth GENCO in pu MW can be expressed in terms of contract participation factors and the total contracted demand of DISCOs as follows:

$$\Delta P_{gm} = cpf_{m1}\Delta P_{L1} + cpf_{m2}\Delta P_{L2} + cpf_{m3}\Delta P_{L3} + cpf_{m4}\Delta P_{L4} \tag{21}$$

where ΔP_{L1}, ΔP_{L2}, ΔP_{L3}, and ΔP_{L4} are the total contracted demands of DISCO1, 2, 3 and 4, respectively.

By using the above equation, the values for ΔP_{gm} can be calculated as follows:

$$\begin{aligned} \Delta P_{g1} &= cpf_{11}P_{L1} + cpf_{12}P_{L2} + cpf_{13}P_{L3} + cpf_{14}P_{L4} \\ &= (0.5) * (0.005) + (0.5) * (0.005) + (0) * (0) + (0) * (0) \\ &= 0.005 \text{ pu MW} \end{aligned} \tag{22}$$

Similarly, the values of ΔP_{g2}, ΔP_{g3}, ΔP_{g4}, ΔP_{g5} and ΔP_{g6} can be obtained as 0.003, 0.002,0, 0 and 0 pu MW respectively.

The final controller parameters of MID controller for the Poolco based transaction are obtained as explained in Section 4.1 and given in Table 1. The performance index in terms of ITAE value, settling times (2% band) and peak overshoot in frequency and tie line power deviations is shown in Table 2. From Table 2, it can be seen that minimum ITAE value is obtained with hDE-PS technique (ITAE = 1.6995) compare to DE technique (ITAE = 1.8503), and GA technique (ITAE = 2.4264). Consequently, better system performance in terms of settling times (2% band) and peak overshoot in frequency and tie-line power deviations is achieved with proposed hDE-PS optimized MID controller compared to other optimization techniques as shown in Table 2. It also clear from Table 2 that peak overshoots in

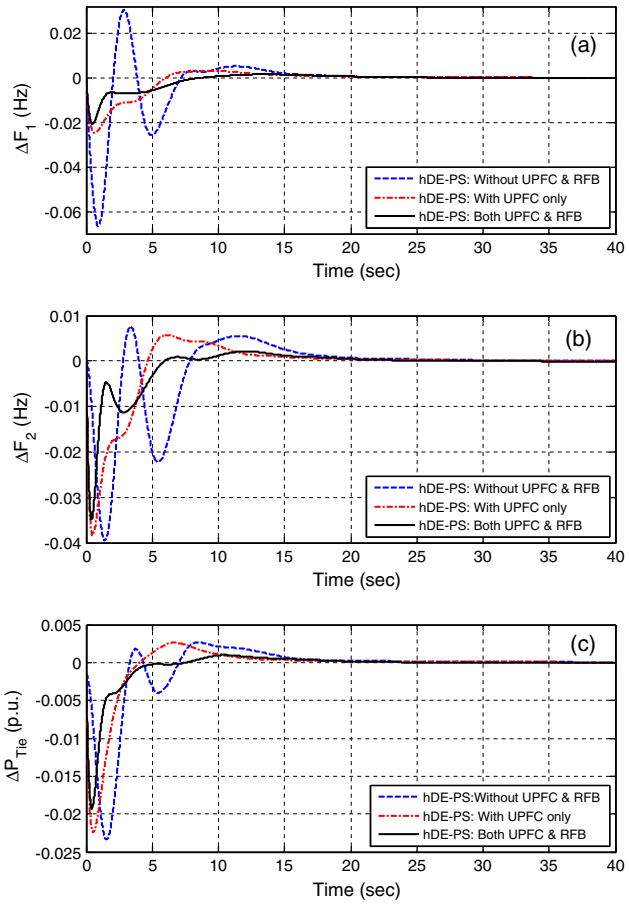

Figure 12 Dynamic responses of the system for contract violation based scenario (a) frequency deviation of area-1 (b) frequency deviation of area-2 (c) tie-line power deviation.

frequency and tie-line responses are greatly reduced by proposed hDE-PS optimized MID controller. The dynamic performance of the system for 1% step increase in load in area-1 under poolco based transaction is shown in Fig. 8a–c. It can be seen from Fig. 8a–c that the system is oscillatory with GA. It is also evident from Fig. 8a–c that oscillations are quickly suppressed with DE optimization technique and best dynamic performance is obtained by proposed hDE-PS optimized MID controller. Hence, the performance of hDE-PS technique is superior to that of DE and GA technique. Hence it can be concluded that for the similar controller structure (MID) and same power system hDE-PS optimization technique outperforms GA and DE techniques.

The performance of proposed hDE-PS optimized MID controller is further investigated for different controller structures such as Integral (I) and Integral Derivative (ID) controllers. The tuned controller parameters of I and ID controller for the Poolco based transaction are obtained as explained in Section 4.1 and provided in Table 3. The ITAE and settling times (2% band) value in frequency and tie line power deviations are also shown in Table 4. For proper comparison the results are compared with I and ID controller for the same power system and optimization technique (hDE-PS). It is observed from Table 4 that, with the same system and optimization technique a less ITAE value is obtained with proposed MID controller (ITAE = 1.6995) compared to ID controller (ITAE = 2.8375) and I controller (ITAE = 3.5887). The overall system performance in terms of settling times and peak over shoots is also greatly improved with proposed MID controller compared to I and ID controller. Therefore it can be concluded that MID controller outperforms I and ID controllers.

Then an UPFC is incorporated in the tie-line to analyze its effect on the power system performance. Finally, Redox Flow Batteries (RFBs) are installed in the area-1 and coordinated with UPFC to study their effect on system performance. A step

Table 10 Sensitive analysis under Poolco based transaction.

Parameter variation	% Change	Settling time in (s)			Peak over shoot $\times 10^{-3}$			ITAE
		ΔF_1	ΔF_2	ΔP_{Tie}	ΔF_1	ΔF_2	ΔP_{Tie}	
Nominal	0	19.07	18.09	12.69	0.8	1.7	0.6	0.3858
Changed DPM		19.13	18.15	12.65	0.7	1.7	0.6	0.3868
Loading Condition	−25	19.07	18.08	12.69	0.8	1.7	0.6	0.3858
	+25	19.08	18.10	12.69	0.8	1.7	0.6	0.3858
T_G	−25	19.08	18.10	12.69	0.8	1.7	0.6	0.3850
	+25	19.06	18.08	12.69	0.8	1.7	0.6	0.3866
T_T	−25	19.12	18.14	12.69	0.7	1.7	0.6	0.3840
	+25	19.02	18.04	12.69	0.8	1.7	0.6	0.3877
T_{GH}	−25	19.17	18.18	12.74	0.8	1.7	0.6	0.3699
	+25	19.00	18.03	12.66	0.8	1.7	0.6	0.4046
T_{12}	−25	19.27	17.69	12.82	0.7	1.9	0.6	0.3895
	+25	18.99	18.33	12.54	0.8	1.6	0.5	0.3832
R	−25	19.20	17.80	13.00	0.7	1.6	0.7	0.3922
	+25	19.09	18.25	12.50	0.8	1.7	0.5	0.3807

Table 11 System eigen values under parameter (loading, T_G and T_T) variation with poolco based transaction.

Loading condition		T_G		T_T	
−25%	+25%	−25%	+25%	−25%	+25%
−2.0000	−2.0000	−2.0000	−2.0000	−2.0000	−2.0000
−0.1000	−0.1000	−0.1000	−0.1000	−0.1000	−0.1000
−0.0205	−0.0205	−0.0205	−0.0205	−0.0205	−0.0205
−2.0000	−2.0000	−2.0000	−2.0000	−2.0	−2.0000
−0.1000	−0.1000	−0.1000	−0.1000	−0.10	−0.1000
−0.0205	−0.0205	−0.0205	−0.0205	−0.0205	−0.0205
−0.1000	−0.1000	−0.1000	−0.1000	−0.1000	−0.1000
−3.3333	−3.3333	−3.3333	−3.3333	−4.4444	−2.6667
−0.1000	−0.1000	−0.1000	−0.1000	−0.1000	−0.1000
−3.3333	−3.3333	−3.3333	−3.3333	−4.4444	−2.6667
−93.2763	−93.2783	−93.2793	−93.2793	−93.2793	−93.2793
−34.4530	−34.4577	−34.4600	−34.4600	−34.4600	−34.4600
−24.4212	−24.4211	−24.4211	−24.4211	−24.4211	−24.4211
−10.1952	−10.1680	−10.1541	−10.1541	−10.1541	−10.1541
−2.3711 ± 2.6382i	−2.3585 ± 2.6584i	−2.3520 ± 2.6686i	−2.3520 ± 2.6686i	−2.3520 ± 2.6686i	−2.3520 ± 2.6686i
−0.7753 ± 0.5419i	−0.1930	−0.1934	−0.1934	−0.1934	−0.1934
−0.8767 ± 0.2503i	−0.7749 ± 0.5400i	−0.7747 ± 0.5390i	−0.7747 ± 0.5390i	−0.7747 ± 0.5390i	−0.7747 ± 0.5390i
−0.1922	−0.8752 ± 0.2517i	−0.8745 ± 0.2524i	−0.8745 ± 0.2524i	−0.8745 ± 0.2524i	−0.8745 ± 0.2524i
−0.1175 ± 0.0432i	−0.1175 ± 0.0432i	−0.1175 ± 0.0432i	−0.1175 ± 0.0432i	−0.1175 ± 0.0432i	−0.1175 ± 0.0432i
−0.1175 ± 0.0432i	−0.1175 ± 0.0432i	−0.1175 ± 0.0432i	−0.1175 ± 0.0432i	−0.1175 ± 0.0432i	−0.1175 ± 0.0432i
−0.0069 ± 0.0090i	−0.0069 ± 0.0090i	−0.0069 ± 0.0090i	−0.0069 ± 0.0090i	−0.0069 ± 0.0090i	−0.0069 ± 0.0090i
−0.0069 ± 0.0090i	−0.0069 ± 0.0090i	−0.0069 ± 0.0090i	−0.0069 ± 0.0090i	−0.0069 ± 0.0090i	−0.0069 ± 0.0090i
−12.5000	−12.5000	−16.6667	−10.0000	−12.5000	−12.5000
−12.5000	−12.5000	−16.6667	−10.0000	−12.5000	−12.5000

Table 12 System eigen values under parameter (T_{GH}, T_{12} and R) variation with poolco based transaction.

T_{GH}		T_{12}		R	
−25%	+25%	−25%	+25%	−25%	+25%
−2.0000	−2.0000	−2.0000	−2.0000	−2.0000	−2.0000
−0.1000	−0.1000	−0.1000	−0.1000	−0.1000	−0.1000
−0.0274	−0.0164	−0.0205	−0.0205	−0.0205	−0.0205
−2.0000	−2.0000	−2.0000	−2.0000	−2.0000	−2.0000
−0.1000	−0.1000	−0.1000	−0.1000	−0.1000	−0.1000
−0.0274	−0.0164	−0.0205	−0.0205	−0.0205	−0.0205
−0.1000	−0.1000	−0.1000	−0.1000	−0.1000	−0.1000
−3.3333	−3.3333	−3.3333	−3.3333	−3.3333	−3.3333
−0.1000	−0.1000	−0.1000	−0.1000	−0.1000	−0.1000
−3.3333	−3.3333	−3.3333	−3.3333	−3.3333	−3.3333
−93.2793	−93.2793	−93.2780	−93.2807	−93.2792	−93.2794
−34.4600	−34.4600	−34.4581	−34.4619	−31.9898	−35.7676
−24.4211	−24.4211	−24.4212	−24.4211	−24.4363	−24.4119
−10.1541	−10.1541	−10.3104	−9.9941	−9.9025	−10.2328
−2.3520 ± 2.6686i	−2.3520 ± 2.6686i	−2.3525 ± 2.6184i	−2.3547 ± 2.7226i	−3.7344 ± 0.3817i	−1.6575 ± 3.0849i
−0.1934	−0.1934	−0.7720 ± 0.4520i	−0.1950	−0.7145 ± 0.5839i	−0.8003 ± 0.5127i
−0.7747 ± 0.5390i	−0.7747 ± 0.5390i	−0.8016 ± 0.2530i	−0.8106 ± 0.5947i	−0.9079 ± 0.2368i	−0.8533 ± 0.2570i
−0.8745 ± 0.2524i	−0.8745 ± 0.2524i	−0.1904	−0.9134 ± 0.2519i	−0.1887	−0.1963
−0.1175 ± 0.0432i	−0.1175 ± 0.0432i	−0.1175 ± 0.0432i	−0.1175 ± 0.0432i	−0.1175 ± 0.0432i	−0.1175 ± 0.0432i
−0.1175 ± 0.0432i	−0.1175 ± 0.0432i	−0.1175 ± 0.0432i	−0.1175 ± 0.0432i	−0.1175 ± 0.0432i	−0.1175 ± 0.0432i
−0.0069 ± 0.0090i	−0.0069 ± 0.0090i	−0.0069 ± 0.0090i	−0.0069 ± 0.0090i	−0.0069 ± 0.0090i	−0.0069 ± 0.0090i
−0.0069 ± 0.0090i	−0.0069 ± 0.0090i	−0.0069 ± 0.0090i	−0.0069 ± 0.0090i	−0.0069 ± 0.0090i	−0.0069 ± 0.0090i
−12.5000	−12.5000	−12.5000	−12.5000	−12.5000	−12.5000
−12.5000	−12.5000	−12.5000	−12.5000	−12.5000	−12.5000

load disturbance of 1% is applied in area-1 and the optimized controller parameters and the corresponding performance index are provided in Table 5. It is clear from Table 5 that, the objective function ITAE value is further reduced to 1.0088 with only UPFC controller and smallest ITAE value (ITAE = 0.3858) is obtained with the coordinated application of UPFC and RFB. The improvements in ITAE value for above cases are 40.64% with IPFC only and 77.3% with

coordinated application of UPFC and RFB compared the system without UPFC and RFB. The performance indexes in terms of settling time and peak overshoots are accordingly reduced. Fig. 9a–c shows the dynamic performance of the system with/without UPFC and RFB for the above disturbance. It can be seen from Fig. 9a–c that the system is oscillatory without UPFC and RFB. The dynamic performance is improved with UPFC and significant improvement in system performance is obtained with coordinated application of UPFC and RFB.

The performance of proposed hDE-PS optimized MID controller is also evaluated under changed contract participation factor. The following modified DPM is considered:

$$\text{DPM} = \begin{bmatrix} 0.4 & 0.4 & 0 & 0 \\ 0.4 & 0.4 & 0 & 0 \\ 0.2 & 0.2 & 0 & 0 \\ 0 & 0 & 0 & 0 \\ 0 & 0 & 0 & 0 \\ 0 & 0 & 0 & 0 \end{bmatrix} \tag{23}$$

The calculated generations under modified DPM are: $\Delta P_{g1} = 0.004$ pu MW, $\Delta P_{g2} = 0.004$ pu MW, $\Delta P_{g3} = 0.002$ pu MW and $\Delta P_{g4} = \Delta P_{g5} = \Delta P_{g6} = 0$ pu MW. A step load disturbance of 1% is applied in area-1 and the corresponding performance indexes are also provided in Table 5. The dynamic performance of the system for the above changed contract participation factor is shown in Fig. 10a–c. It can be seen from Table 5 and Fig. 10a–c that the proposed controller is robust and performs satisfactorily with change of contract participation factor.

4.3. Bilateral based transaction

In this scenario, DISCOs have the freedom to contract with any of the GENCOs within or with other areas and it is assumed that a step load disturbance of 0.005 pu MW is demanded by each DISCO in both areas *i.e.* $\Delta P_{L1} = 0.005$ pu MW, $\Delta P_{L2} = 0.005$ pu MW, $\Delta P_{L3} = 0.005$ pu MW and $\Delta P_{L4} = 0.005$ pu MW as result of the total load disturbance in area-1 is $\Delta P_{D1} = 0.01$ pu MW and in area-2 is $\Delta P_{D2} = 0.01$ pu MW.

From Eq. (3) the deviation in scheduled tie-line power is 0.0015 pu MW. All the GENCOs are participating in the LFC task as per the following DPM.

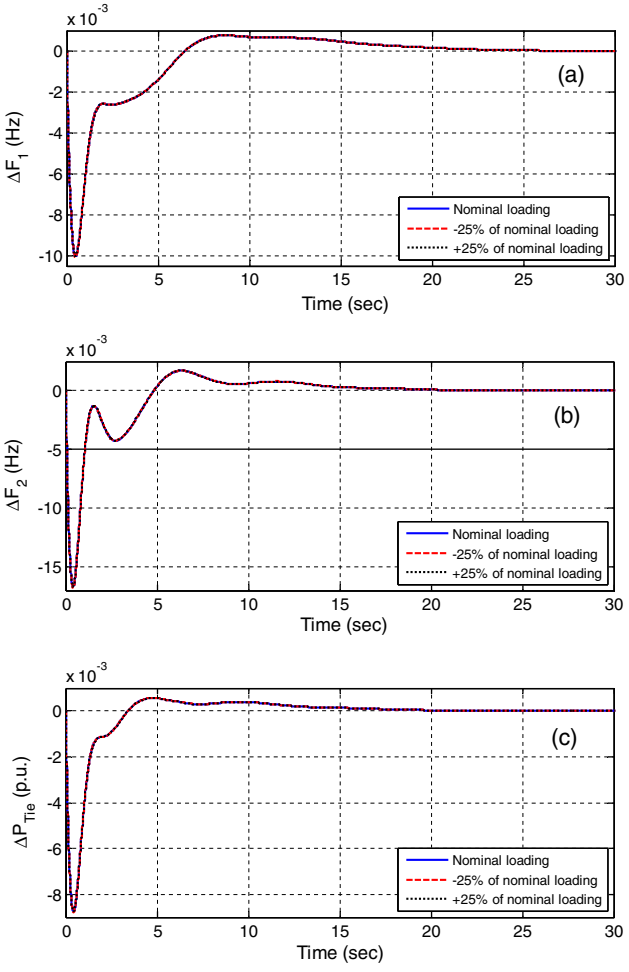

Figure 13 Dynamic responses of the system with variation of loading condition (a) frequency deviation of area-1 (b) frequency deviation of area-2 (c) tie-line power deviation.

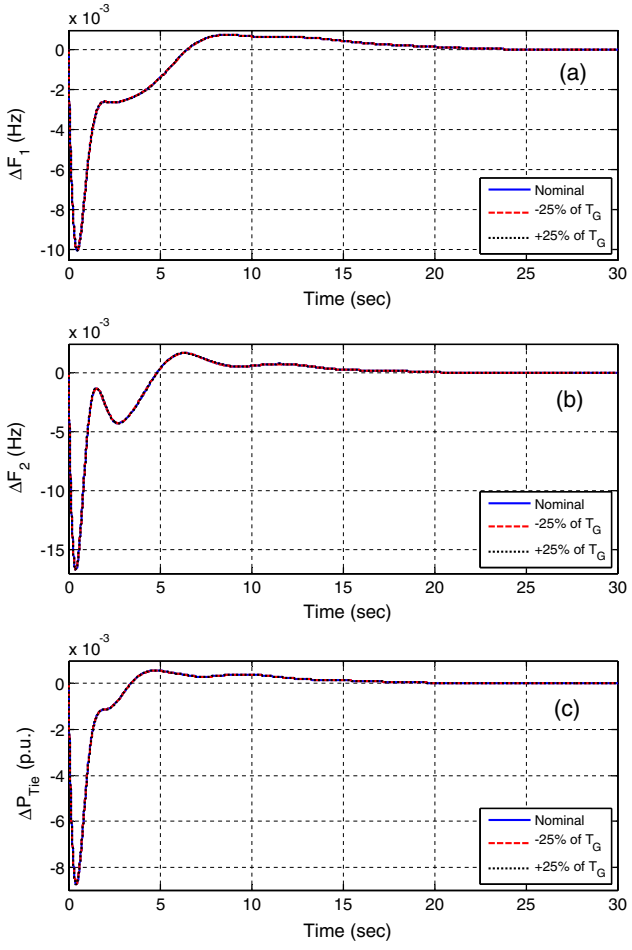

Figure 14 Dynamic responses of the system with variation of T_G (a) frequency deviation of area-1 (b) frequency deviation of area-2 (c) tie-line power deviation.

$$\text{DPM} = \begin{bmatrix} 0.2 & 0.1 & 0.3 & 0 \\ 0.2 & 0.25 & 0.1 & 0.1666 \\ 0.1 & 0.25 & 0.1 & 0.1666 \\ 0.2 & 0.1 & 0.1 & 0.3666 \\ 0.2 & 0.2 & 0.2 & 0.1666 \\ 0.1 & 0.1 & 0.2 & 0.1666 \end{bmatrix} \quad (24)$$

From Eq. (21) the values of steady-state power generated by the GENCOs can be obtained as: $\Delta P_{g1} = 0.003$ pu MW, $\Delta P_{g2} = 0.0036$ pu MW, $\Delta P_{g3} = 0.0031$ pu MW, $\Delta P_{g4} = 0.0038$ pu MW, $\Delta P_{g5} = 0.0038$ pu MW and $\Delta P_{g6} = 0.0028$ pu MW.

The tuned MID controller parameters for Bilateral based transaction are given in Table 6. The various performance indexes (ITAE, settling time and peak overshoot) under bilateral based transaction case are given in Table 7. It is clear from Table 7 that minimum ITAE value is obtained with coordinated application of UPFC and RFB (ITAE = 0.5033) compared to only UPFC (ITAE = 1.0331) and without UPFC and RFB optimized MID controller (ITAE = 2.0231). The improvements in ITAE value for above case are 48.93% with UPFC only and 75.12% with coordinated application of UPFC and RFB. Consequently, better system performance in terms of minimum settling times in frequency and tie-line power deviations is achieved with proposed UPFC and RFB optimized MID controller compared to others as shown in Table 7. Hence it can be concluded that in this case also, the coordination of IPFC and RFB works satisfactorily. The system dynamic responses are shown in Fig. 11a–c. From Fig. 11a–c, it shows that coordinated application of UPFC and RFB significantly improves the dynamic performance of the system. Improved results in settling times and peak overshoots of ΔF_1, ΔF_2 and ΔP_{Tie} are obtained with proposed hDE-PS optimized MID controller with coordinated application of UPFC and RFB compared to others.

4.4. Contract violation

It may happen that DISCOs may violate a contract by demanding more than that specified in the contract. This excess power is not contracted out to any GENCO. This uncontracted power must be supplied by the GENCOs in the same area as that of the DISCOs. It must be reflected as a local load of the area but not as the contract demand. Considering scenario 2 (bilateral based transaction) again with a modification that 0.01 (pu MW) of excess power demanded by

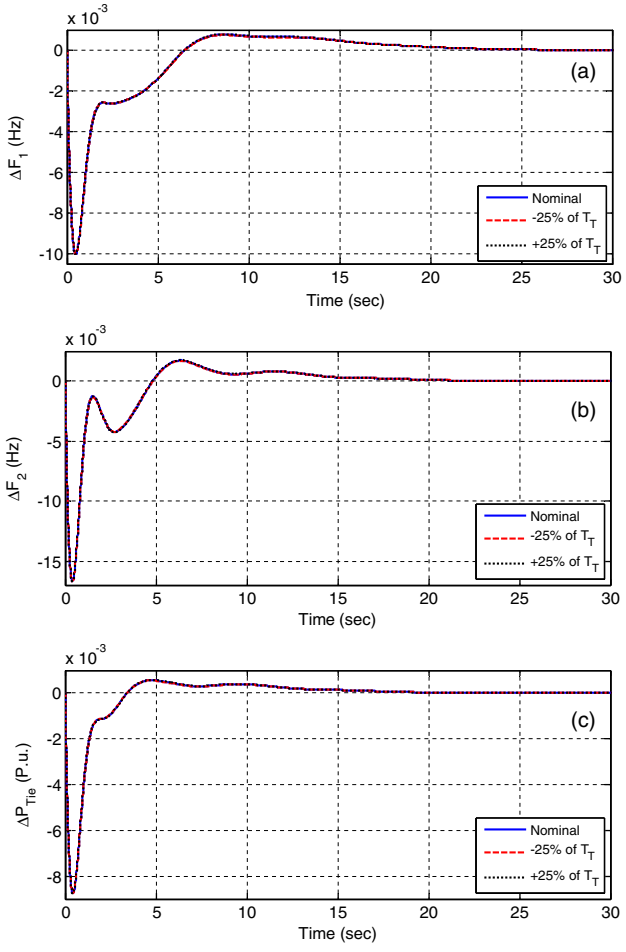

Figure 15 Dynamic responses of the system with variation of T_T (a) frequency deviation of area-1 (b) frequency deviation of area-2 (c) tie-line power deviation.

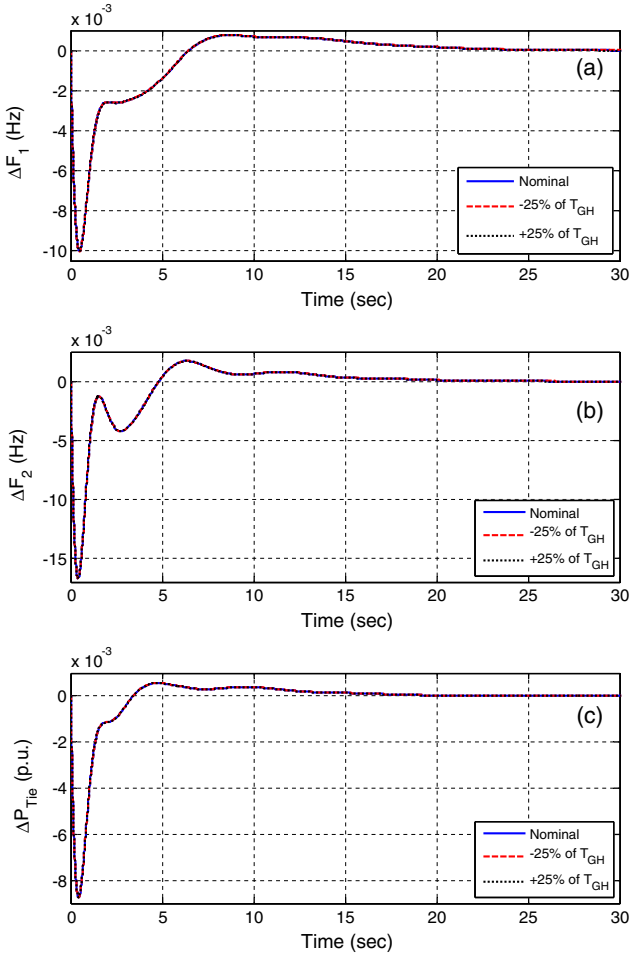

Figure 16 Dynamic responses of the system with variation of T_{GH} (a) frequency deviation of area-1 (b) frequency deviation of area-2 (c) tie-line power deviation.

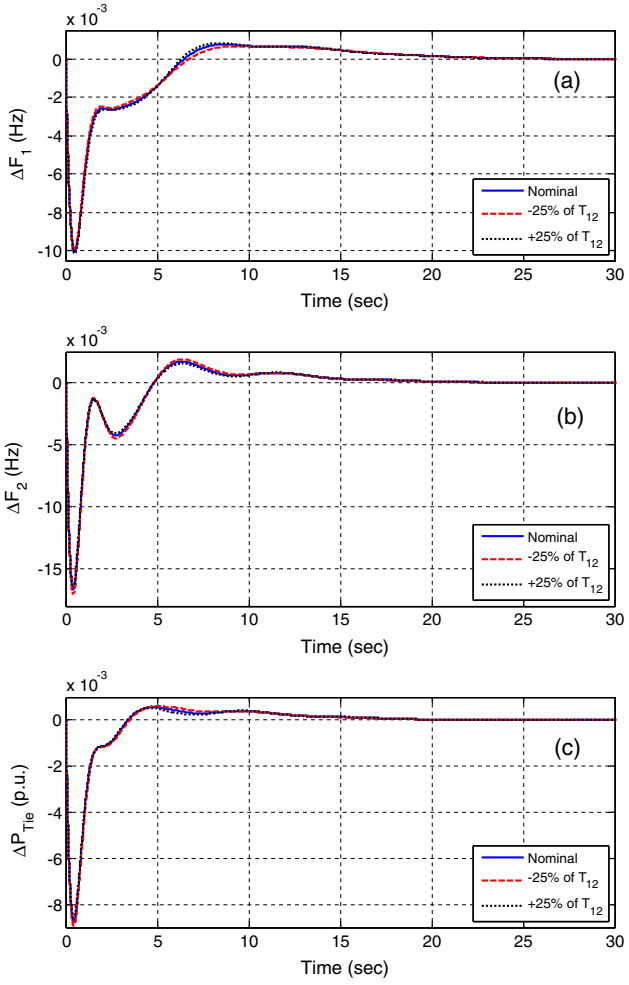

Figure 17 Dynamic responses of the system with variation of T_{12} (a) frequency deviation of area-1 (b) frequency deviation of area-2 (c) tie-line power deviation.

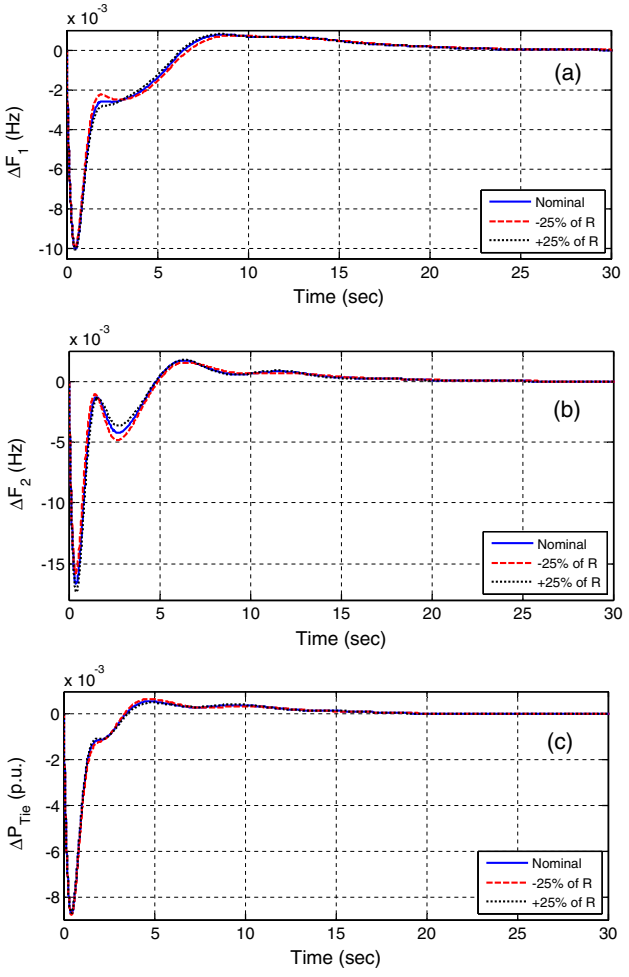

Figure 18 Dynamic responses of the system with variation of R (a) frequency deviation of area-1 (b) frequency deviation of area-2 (c) tie-line power deviation.

DISCO1. Now ΔP_{D1} becomes, $\Delta P_{D1} = \Delta P_{L1} + \Delta P_{L2} + \Delta P_{uc1} = 0.02$ (pu MW) while ΔP_{D2} remains unchanged. As there is contract violation, the values of ΔP_{g1}, ΔP_{g2} and ΔP_{g3} are to be changed. The change in violation of powers calculated as follows:

$$\Delta P_{g1,violation} = \Delta P_{g1} + apf_{11}{}^{*}\Delta P_{violation} = 0.009 \text{ p.u MW} \quad (25)$$

$$\Delta P_{g2,violation} = \Delta P_{g2} + apf_{12}{}^{*}\Delta P_{violation} = 0.0066 \text{ pu MW} \quad (26)$$

$$\Delta P_{g3,violation} = \Delta P_{g3} + apf_{13}{}^{*}\Delta P_{uc1} = 0.0041 \text{ pu MW} \quad (27)$$

The values of ΔP_{g4}, ΔP_{g5} and ΔP_{g6} are same as in scenario 2 (bilateral based transaction).

Table 8 gives the tuned MID controller parameters for contract violation based transaction. The various performance indexes in terms of ITAE, settling time and peak overshoot for the above case are given in Table 9. It can be seen from Table 9 that superior results are obtained with coordinated application of UPFC and RFB compared to others. The improvements in ITAE value for contract violation based transaction are 36.91% with UPFC only and 64.78% with coordinated application of UPFC and RFB. The frequency deviations and tie-line power are shown in Fig. 12a–c. It is evident from Fig. 12a–c that with coordinated application of UPFC and RFB the oscillations are quickly damped out.

4.5. Sensitivity analysis

Robustness is the ability of a system to perform effectively while its variables are changed within a certain tolerable range [21,26,28]. In this section robustness of the power system is checked by varying the loading conditions and system parameters from their nominal values (given in Appendix A) in the range of +25% to −25% without changing the optimum values of proposed MID controller gains. The change in operating load condition affects the power system parameters K_{PS} and T_{PS}. The power system parameters are calculated for different loading conditions as given in Appendix A. The system with UPFC and RFB under poolco based scenario is considered in all the cases due to their superior performance. The various performance indexes (ITAE values, settling times and peak overshoot) under normal and parameter variation cases for the system are given in Table 10. It can be observed from Table 10 that the ITAE, settling time and peak overshoot values are varying within acceptable ranges and are nearby equal to the respective values obtained with nominal system parameter. The system modes under these cases are shown in Tables 11 and 12. It is also evident from Tables 11 and 12 that the eigen values lie in the left half

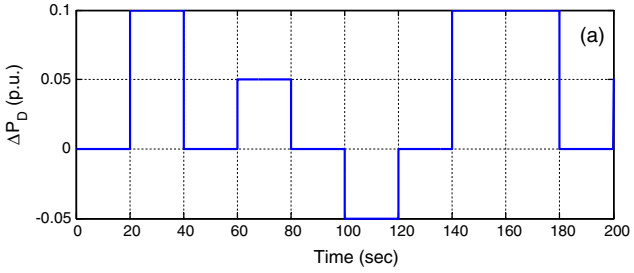

Figure 19a Random step load pattern varied from −0.05 pu to 0.1 pu.

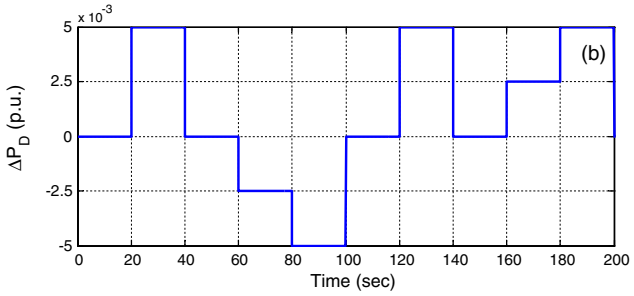

Figure 19b Random step load pattern varied from −0.005 pu to 0.005pu.

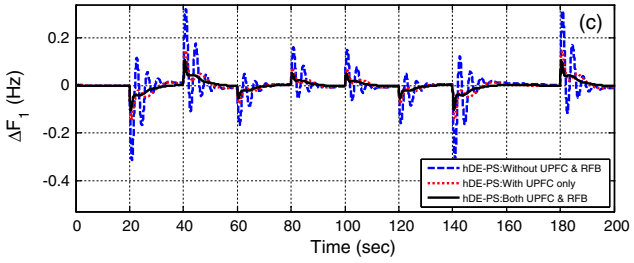

Figure 19c Frequency deviation in area-1 under poolco based scenario for random load pattern varied from −0.05 to 0.1 pu.

of s-plane for all the cases thus maintain the stability [26,28,29,30]. Hence, it can be concluded that the proposed MID controller in deregulation environment is very much robust and performs satisfactorily when system parameters changes in the range of ±25%.

The dynamic performances of the system under variation of parameters are shown in Figs. 13–18. It can be observed from Figs. 13–18 that the effect of the variation of operating loading conditions on the system responses is negligible. Hence it can be concluded that, the proposed control strategy provides a robust control under wide changes in the loading condition and system parameters. Further, to investigate the superiority of the proposed method, a random step load changes are applied in area-1 i.e. under poolco based scenario. Figs. 19a and 19b show the random load pattern of power system. The step loads are random both in magnitude and duration. The frequency response for random load disturbance in area-1 is shown in Figs. 19c and 19d. From Figs. 19c and 19d, it is evident that proposed method shows better transient

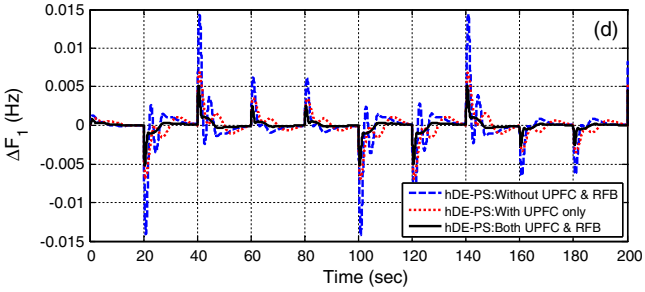

Figure 19d Frequency deviation in area-1 under poolco based scenario for random load pattern varied from −0.005 to 0.005pu.

response when the system is incorporated with UPFC and RFB than other.

It is worth mentioning that, the controllers are designed offline during planning stage and then put into action for online control of power system. So before the controllers are put into operation, the parameters are determined and they remain fixed. Therefore, the complexity of using proposed hybrid method to determine the controller parameters will not increase the computational burdens during online applications.

5. Conclusion

In this paper, an attempt has been made for the first time to apply a hybrid Differential Evolution (DE) and Pattern Search (PS) optimized Modified Integral Derivative (MID) controller for load frequency control of multi-area multi-source power system in deregulated environment. The Boiler dynamics, Generation Rate Constraint (GRC) and Governor Dead Band (GDB) have been considered to have a more realistic power system. The system has been investigated all possible of power transactions that take place under deregulated environment. The proposed hybrid technique takes advantage of global exploration capabilities of DE and local exploitation capability of PS. The advantage of proposed hDE-PS technique over DE and Genetic Algorithm (GA) has also been demonstrated. It is observed that better dynamic performance is obtained with proposed hDE-PS optimized MID controller compared to I and ID controller. Unified Power Flow Controller (UPFC) is added in the tie-line for improving the system performance. Additionally, Redox Flow Batteries (RFBs) are included in area-1 along with UPFC in order to improve the system performance. It is observed that in all the cases (poolco based, bilateral based and contract violation based) the deviation of frequency becomes zero in the steady state with coordinated application of UPFC and RFB which assures the AGC requirements. Additionally, sensitivity analysis is carried out to show the robustness of the MID controller under poolco based scenario. From simulation results, it is observed that the parameters of the proposed hDE-PS optimized MID controllers are need not be reset even if the system is subjected to wide variation in loading condition and system parameters. Finally, the simulation results are demonstrated that the proposed approach provides desirable performance against random step load disturbance.

Appendix A

Nominal parameters of the system investigated are as follows:

A.1. Two area multisource thermal hydro wind diesel power system [19]

$F = 60$ Hz; $B_1 = B_2 = 0.425$ p.u.MW/Hz; $R_1 = R_2 = R_3 = R_4 = R_5 = R_6 = 2.4$ Hz/p.u.; $T_{G1} = T_{G2} = 0.08$ s; $T_{T1} = T_{T2} = 0.3$ s; $K_{r1} = K_{r2} = 0.333$, $T_{r1} = T_{r2} = 10$ s, $T_{GH1} = T_{GH2} = 48.7$ s; $T_{RS1} = T_{RS2} = 0.513$; $T_{RH1} = T_{RH2} = 10$; $T_{W1} = 1$; $K_{diesel} = 16.5$; $K_{P1} = 1.25$; $K_{P2} = 1.4$; $T_{P1} = 6$; $T_{P2} = 0.041$; $K_1 = 0.85$; $K_2 = 0.095$; $K_3 = 0.92$; $K_{IB} = 0.03$; $T_{IB} = 26$; $T_{RB} = 6.9$; $C_B = 200$; $T_D = 0$; $T_F = 10$; $K_{PS1} = K_{PS2} = 120$ Hz/p.u.MW; $T_{PS1} = T_{PS2} = 20$ s; $T_{12} = 0.0866$ pu; $a_{12} = -1$.

A.2. Data for UPFC & RFB

$T_{\mathrm{UPFC}} = 0.01$ s; $K_{\mathrm{RFB}} = 0.67$; $T_{\mathrm{RFB}} = 0$ s.

References

[1] Elgerd OI. Electric energy systems theory – an introduction. New Delhi: Tata McGraw Hill; 2000.
[2] Bevrani H. Robust power system frequency control. Springer; 2009.
[3] Bervani H, Hiyama T. Intelligent automatic generation control. CRC Press; 2011.
[4] Donde V, Pai MA, Hiskens IA. Simulation and optimization in an AGC system after deregulation. IEEE Trans Power Syst 2011;16:481–9.
[5] Christie RD, Bose A. Load frequency control issues in power system operation after deregulation. IEEE Trans Power Syst 1996;11:1191–2000.
[6] Parmar KPS, Majhi S, Kothari DP. LFC of an interconnected power system with multi-source power generation in deregulated power environment. Int J Elect Power Energy Syst 2014;57:277–86.
[7] Debbarma S, Saikia LC, Sinha N. AGC of a multi-area thermal system under deregulated environment using a non-integer controller. Electric Power Syst Res 2013;95:175–83.
[8] Demiroren A, Zeynelgil HL. GA application to optimization of AGC in three-area power system after deregulation. Int J Elect Power Energy Syst 2007;29:230–40.
[9] Bhatt P, Roy R, Ghoshal SP. Optimized multi area AGC simulation in restructured power systems. Int J Elect Power Energy Syst 2010;32:311–32.
[10] Saikia LC, Nanda J, Sinha N. Performance comparison of several classical controllers in AGC for multi-area interconnected thermal system. Int J Elect Power Energy Syst 2011;33:394–401.
[11] Tan W, Zhang H, Yu M. Decentralized load frequency control in deregulated environments. Int J Elect Power Energy Syst 2012;41:16–26.
[12] Liu F, Song YH, Ma J, Mei S, Lu Q. Optimal load–frequency control in restructured power systems. IEE Proc Gen Trans Distribution 2003;150(1):87–95.
[13] Das D, Aditya SK, Kothari DP. Dynamics of diesel and wind turbine generators on an isolated power system. Int J Elect Power Energy Syst 1999;21:183–9.
[14] Hingorani NG, Gyugyi L. Understanding FACTS: concepts and technology of flexible AC transmission system. IEEE Press; 2000.
[15] Sasaki T, Kadoya T, Kazuhiro E. Study on load frequency control using redox flow batteries. IEEE Trans Power Syst 2004;19(1):660–7.
[16] Enomoto K, Sasaki T, Shigematsu T, Deguchi H. Evaluation study about redox flow battery response and its modelling. IEEJ Trans Power Eng 2002;122(4):554–60.
[17] Chidambaram IA, Paramasivam B. Optimized load–frequency simulation in restructured power system with redox flow batteries and interline power flow controller. Int J Elect Power Energy Syst 2013;50:9–24.
[18] Dolan ED, Lewis RM, Torczon V. On the local convergence of pattern search. SIAM J Optimiz 2003;14(2):567–83.
[19] Mohanty B, Panda S, Hota PK. Differential evolution algorithm based automatic generation control for interconnected power systems with non-linearity. Alexandria Eng J 2014;53(3):537–52.
[20] Khuntia SR, Panda S. Simulation study for automatic generation control of a multi-area power system by ANFIS approach. Appl Soft Comput 2012;12(1):333–41.
[21] Sahu RK, Panda S, Padhan S. Optimal gravitational search algorithm for automatic generation control of interconnected power systems. Ain Shams Eng J 2014;5(3):721–33.
[22] Panda S. Robust coordinated design of multiple and multi-type damping controller using differential evolution algorithm. Int J Elect Power Energy Syst 2011;33:1018–30.
[23] Kazemi A, Shadmesgaran MR. Extended supplementary Controller of UPFC to improve damping inter-area oscillations considering inertia coefficient. Int J Energy 2008;2(1):25–36.
[24] Parmar KPS. Load frequency control of multi-source power system with redox flow batteries: an analysis. Int J Computer Appl 2014;88(8):46–52.
[25] Stron R, Price K. Differential evolution – a simple and efficient adaptive scheme for global optimization over continuous spaces. J Global Optimiz 1995;11:341–59.
[26] Sahu RK, Panda S, Rout UK. DE optimized parallel 2-DOF PID controller for load frequency control of power system with governor dead-band nonlinearity. Int J Elect Power Energy Syst 2013;49(1):19–33.
[27] Othman AK, Ahmed AN, AlSharidah ME, AlMekhaizim HA. A hybrid real coded genetic algorithm – pattern search approach for selective harmonic elimination of PWM AC/AC voltage controller. Int J Elect Power Energy Syst 2013;44:123–33.
[28] Rout UK, Sahu RK, Panda S. Design and analysis of differential evolution algorithm based automatic generation control for interconnected power system. Ain Shams Eng J 2013;4(3):409–21.
[29] Debbarma S, Saikia LC, Sinha N. Automatic generation control using two degree of freedom fractional order PID controller. Int J Elect Power Energy Syst 2014;58:120–9.
[30] Ali ES, Abd-Elazim SM. Bacteria foraging optimization algorithm based load frequency controller for interconnected power system. Int J Elect Power Energy Syst 2011;33(3):633–8.

Rabindra Kumar Sahu received the Ph.D. degree from the Indian Institute of Technology (IIT) Madras, Chennai, India. He is currently working as Associate Professor and Head of the Department, Electrical Engineering & EEE, Veer Surendrai Sai University of Technology (VSSUT), Burla, Sambalpur, Odisha, India. His research interests include application of soft computing techniques to power system engineering, Flexible AC Transmission Systems (FACTS). Dr. Sahu is a life member of ISTE.

G.T. Chandra Sekhar received B.Tech degree in EEE from St. Theressa institute of Engineering & Technology, Vizianagaram affiliated to JNTU, Hyderabad, Andhra Pradesh in 2008. M.Tech Degree in EEE from St. Theressa institute of Engineering & Technology, Vizianagaram affiliated to JNTU, Kakinada, Andhra Pradesh in 2011. He is currently working toward the Ph.D. degree at the Department of Electrical Engineering, VSSUT, Burla, Odisha, India. His research interests include soft computing application in power system Engineering. Mr. Chandra Sekhar is a life member of ISTE.

Sidhartha Panda received Ph.D. degree from Indian Institute of Technology (IIT), Roorkee, India, M.E. degree from Veer Surendrai Sai University of Technology (VSSUT). Presently, he is working as a Professor in the Department of Electrical Engineering, Veer Surendrai Sai University of Technology (VSSUT), Burla, Sambalpur, Odisha, India. His areas of research include Flexible AC Transmission Systems (FACTS), Power System Stability, Soft computing, Model Order Reduction, Distributed Generation and Wind Energy. Dr. Panda is a Fellow of Institution of Engineers (India).